Ferromagnetic domains in the large- U Hubbard model with a few holes: A full configuration interaction quantum Monte Carlo study

Ferromagnetic domains in the large-U Hubbard model with a few holes: A full configuration interaction quantum Monte Carlo study

Sujun Yun [*]
Max Planck Institute for Solid State Research, Heisenbergstraße 1, 70569 Stuttgart, Germany and School of Electronic Engineering, Nanjing XiaoZhuang University, Hongjing Road, Nanjing 211171, China

Werner Dobrautz [†]
Department of Chemistry and Chemical Engineering, Chalmers University of Technology, 41296 Gothenburg, Sweden

Hongjun Luo [‡], Vamshi Katukuri, and Niklas Liebermann
Max Planck Institute for Solid State Research, Heisenbergstraße 1, 70569 Stuttgart, Germany

Ali Alavi [§]
Max Planck Institute for Solid State Research, Heisenbergstraße 1, 70569 Stuttgart, Germany and Yusuf Hamied Department of Chemistry, University of Cambridge, Lensfield Road, Cambridge CB2 1EW, United Kingdom

(Received 25 October 2022; accepted 23 December 2022; published 7 February 2023)

Two-dimensional Hubbard lattices with two or three holes are investigated as a function of U in the large-U limit. In the so-called Nagaoka limit (one-hole system at infinite U), it is known that the Hubbard model exhibits a ferromagnetic ground state. Here, by means of exact full configuration interaction quantum Monte Carlo simulations applied to periodic lattices up to 24 sites, we compute spin-spin correlation functions as a function of increasing U. The correlation functions clearly demonstrate the onset of ferromagnetic domains, centered on individual holes. The overall total spin of the wave functions remains the lowest possible (0 or $\frac{1}{2}$, depending on the number of holes). The ferromagnetic domains appear at interaction strengths comparable to the critical interaction strengths of the Nagaoka transition in finite systems with strictly one hole. The existence of such ferromagnetic domains is the signature of Nagaoka physics in Hubbard systems with a small (but greater than 1) number of holes.

DOI: 10.1103/PhysRevB.107.064405

I. INTRODUCTION

The Hubbard model is a simple yet important model in the study of correlated electrons, as it captures complex correlations between electrons on a lattice with a fairly simple Hamiltonian [1]. Exact results of the two-dimensional Hubbard model are helpful for understanding a plethora of phenomena in strongly correlated systems, including pairing mechanisms in unconventional superconductors [2], the Mott metal-insulator transition [3], optical conductivity [4,5], and itinerant magnetism [6,7]. For the single-band 2D Hubbard model on a square lattice, Nagaoka [8] proved analytically that the limit of infinitely strong interactions, in the presence of a single hole on top of a Mott-insulating state with one electron per site, results in a ferromagnetic ground state. Intuitively, the Nagaoka ferromagnetism can be understood as resulting from an interference effect between the different paths that the hole can take across the lattice. When the spins are aligned, these paths interfere constructively and lower the kinetic energy of the hole [9–12].

While Nagaoka ferromagnetism has been analytically proven under extreme conditions, and has also been observed in a quantum dot plaquette [13], the stability of the Nagaoka ferromagnetic state at finite interaction strengths on finite lattices has also been actively studied [14–21]. However, open questions still exist, especially concerning the thermodynamic stability of the ferromagnetic state for systems with more than one hole. Extrapolations from the results on finite lattices have been used to study properties in the thermodynamic limit. Thus it is important to obtain exact results in systems with two, three, and perhaps more holes, on lattices as large as possible.

In the two-hole system, the total spin of the ground state is zero ($S = 0$). This has been numerically studied by exact diagonalization (ED) [22], the spin-adapted full configuration interaction quantum Monte Carlo (FCIQMC) method [21],

[*]yunsujun@163.com
[†]dobrautz@chalmers.se
[‡]h.luo@fkf.mpg.de
[§]a.alavi@fkf.mpg.de

TABLE I. The ground-state $S = 0$ spin-spin correlation $\langle \mathbf{S}(i) \cdot \mathbf{S}(j) \rangle$ values as a function of their distance, $R = |i - j|$, obtained from FCIQMC calculations on the 18-site square lattice Hubbard model with 16 electrons for different values of U. For comparison the values from the exact diagonalization (ED) calculation taken from Ref. [42] are also shown.

	$R = 1$		$R = \sqrt{2}$		$R = 2$		$R = \sqrt{5}$		$R = 3$	
U	2-RDM	ED	2-RDM	ED	2-RDM	ED	2-RDM	ED	2-RDM	ED
20	−0.1910(1)	−0.19096	0.0448(1)	0.04473	−0.0154(1)	−0.01541	−0.01401(1)	−0.01398	0.0493(1)	0.04931
40	−0.1820(1)	−0.18197	0.0341(1)	0.03417	−0.0274(1)	−0.02739	−0.0062(1)	−0.0061	0.0619(1)	0.06188

and analytical studies of arbitrarily large systems [19]. However, the specific type of magnetism is unknown, because antiferromagnetism, paramagnetism, as well as low-spin-coupled ferromagnetic domains all correspond to $S = 0$. For the three-hole system, on the other hand, ED results of an effective Hamiltonian [22] show that the total spins of ground states on the 8- and 16-site lattices are $\frac{3}{2}$ and $\frac{7}{2}$, respectively. Here the effective Hamiltonian is constructed to exclude double occupation and thus should be related to the Hubbard model in the large-U limit. It is interesting to see whether the partial magnetization will still be observed on larger lattices. In order to answer the above open questions, in this work we investigate the two- and three-hole systems with the FCIQMC method.

FCIQMC is based on stochastic simulations of the dynamic evolution of the wave function in imaginary time. Different from the diffusion quantum Monte Carlo (DMC) [23] with the fixed-node approximation and the auxiliary-field quantum Monte Carlo (AFQMC) [24] with the phaseless approximation, no systematic approximation is made in FCIQMC [25–27], and it thus serves as a highly accurate method to approach the ground-state wave functions. The annihilation procedure of the algorithm enables it to overcome the fermionic sign problem exactly, as long as enough walkers are used to overcome the annihilation plateau which is observed in the method [25]. In practice, for Hubbard systems at large U, this means, with the currently available hardware, systems up to 26 sites can be studied [21]. (A 26-site lattice represents a useful increase in size compared to exact diagonalization, for which 20 sites is the largest lattice size so far reported [4].) In the present paper, we extend this to the study of a system with a few holes, as well as report on spin-spin correlation functions for the obtained exact ground states.

The energy in FCIQMC is most easily calculated through projection onto an appropriate trial wave function Ψ^T,

$$E_{\text{proj}} = \frac{\langle \Psi^T | \hat{H} | \Psi \rangle}{\langle \Psi^T | \Psi \rangle}, \tag{1}$$

where Ψ is the wave function given by the instantaneous distribution of walkers. Clearly, for this expression to be useful, the denominator needs to have a nonzero time average, with small fluctuations. In practice, this requirement is fulfilled when a sufficient number of walkers is used to overcome the annihilation plateau, meaning that at least one determinant acquires a permanent population of walkers of a given sign. This fixes the global sign of Ψ, and leads to a substantially nonzero time average of $\langle \Psi^T | \Psi \rangle$. Nevertheless, it should be noted that even after this has occurred, the projected energy fluctuates [as both the numerator and denominator of Eq. (1) are stochastic quantities], and for this reason, the instantaneous value of E_{proj} can dip below the exact energy. However, the time average of the projected energy converges to the exact FCI energy within stochastic error bars [25], which can estimated through a reblocking analysis of the time sequences of the numerator and denominator of the projected energy formula [27]. In Table I of the Supplemental Material [44], the total energies (showing stochastic errors of about $10^{-3}t$) are provided for the systems studied in this paper.

The FCIQMC simulations were performed with the NECI package code base, which provides a state-of-the-art implementation of the FCIQMC algorithm, and a very powerful parallelization which scales efficiently to more than 24 000 central processing unit cores [27]. The FCIQMC method in a Slater determinant (SD) basis has been extended to calculate ground and excited state energies, spectral and Green's functions for *ab initio* and model systems, as well as properties via the one-, two-, three-, and four-body reduced density matrices (RDMs). To study magnetism, we need to use the replica-sampled 2-RDMs [28–30] to obtain the spatial spin distribution. The replica-sampling technique removes the systematic error in the RDM, at the expense of requiring a second walker distribution. The premise is to ensure that these two walker distributions are entirely independent and propagated in parallel, sampling the same (in this instance ground state) distribution. This ensures an unbiased sampling of the desired RDM, by ensuring that each RDM contribution is derived from the product of an uncorrelated amplitude from each replica walker distribution. By using replica-sampled 2-RDMs the spin-spin correlation function, $\langle \hat{\mathbf{S}}_i \cdot \hat{\mathbf{S}}_j \rangle$, can be calculated, where i and j are lattice site indices. This spin-spin correlation function can then be used to identify the specific type of magnetism of the ground states.

FCIQMC in a spin-adapted basis is also used to study the partial polarization in three-hole systems. Spin-adapted FCIQMC uses $SU(2)$ symmetry (arising from the vanishing commutator $[\hat{H}, \hat{\mathbf{S}}^2] = 0$) conservation. $SU(2)$ symmetry is imposed via the graphical unitary group approach (GUGA) [31–33] which dynamically constrains the total spin S of a multiconfiguration and highly open-shell wave function in an efficacious manner. The spin-adapted version of the FCIQMC algorithm based on GUGA has been developed in our group [34,35], with—among others—applications to *ab initio* systems [36,37] and Nagaoka ferromagnetism in one-hole systems [21]. With the spin-adapted method, the magnetization of the ground state can be determined in a reliable way, especially for systems with small spin gaps. The results of spin-adapted FCIQMC show the partial spin

polarization only appears in small, three-hole system (less than 18 sites) [22], which is the second important result of this work.

The rest of this paper is organized as follows: In Sec. II, we briefly describe the methods, where we mainly provide some more details on the measurements of the spin-spin correlation function, $\langle \hat{\mathbf{S}}_i \cdot \hat{\mathbf{S}}_j \rangle$, from the replica-sampled 2-RDMs in FCIQMC. In Sec. III, results about the spatial spin distribution and partial spin polarization are discussed. Finally, we conclude in Sec. IV.

II. METHODS

The Hamiltonian of the Hubbard model in real space takes the form

$$\hat{H} = -t \sum_{\langle ij \rangle \sigma} a^\dagger_{i,\sigma} a_{j,\sigma} + U \sum_i n_{i\uparrow} n_{i\downarrow}, \tag{2}$$

where $a^\dagger_{i\sigma}$ ($a_{i\sigma}$) creates (annihilates) an electron with spin σ on site i, and $n_{i\sigma} = a^\dagger_{i\sigma} a_{i\sigma}$ is the particle number operator. U refers to the Coulomb interaction strength. We consider only nearest-neighbor hopping terms, where t is positive and is used as the unit of the energy. When U is infinitely large, there will be no double occupancy and the system can be treated with an effective Hamiltonian with constrained hopping terms [22]

$$H_{\text{eff}} = -t \sum_{\langle ij \rangle \sigma} \tilde{a}^\dagger_{i,\sigma} \tilde{a}_{j,\sigma}, \tag{3}$$

with $\tilde{a}^\dagger_{i,\sigma} = a_{i,\sigma}(1 - n_{i,\sigma})$. In our current work, we want to study the magnetic properties for finite U and thus will stay with the original Hamiltonian (2). However, we find that our results for the three-hole systems in the large-U limit (see Sec. III B) coincide with the result of Riera *et al.* [22] for the effective Hamiltonian, Eq. (3). In future work we will study the t-J model [38], containing corrections of order t^2/U [39] to study ferromagnetic domains for larger lattices. In our current investigation we apply two different FCIQMC methods, which are based on full CI expansions in terms of SDs and in terms of spin eigenfunctions (spin-adapted basis states), respectively.

FCIQMC is a projector QMC method for obtaining the ground-state wave function $|\Psi_0\rangle$. By Monte Carlo simulation of the imaginary-time evolution of the wave function

$$|\Psi(\tau)\rangle = e^{-\tau(\hat{H} - E_0)} |\Psi(0)\rangle, \tag{4}$$

the ground-state wave function is approached in the long-time limit $|\Psi(\tau \to \infty)\rangle \propto |\Psi_0\rangle$.

In a previous work [21], we have investigated the magnetism for one-hole and two-hole systems by using the spin-adapted [$SU(2)$ conserving] FCIQMC method. We extend these investigations to three-hole systems in this work. With the spin-adapted method, the magnetization of the ground state can be determined in a reliable way, especially for systems with small spin gaps. For details of the spin-adapted FCIQMC method, we refer to previous work [21].

We also calculate the spin-spin correlation function to get knowledge of the spatial spin distribution. For these calculations, we find that the FCIQMC method based on SDs is more efficient, in particular when it is combined with the replica-sampling techniques for the 2-RDMs. With this technique, two independent FCIQMC simulations are performed in parallel and the wave function expansions

$$|\Psi(\tau)^{I/II}\rangle = \sum_\mu c^{I/II}_\mu(\tau) |D_\mu\rangle \tag{5}$$

are sampled simultaneously for these two replicas. The sampled coefficients $\{c^I_\mu\}$ and $\{c^{II}_\mu\}$ are then used to calculate the 2-RDM elements

$$\begin{aligned} \Gamma^{rs}_{pq} &= \langle \Psi | a^\dagger_p a^\dagger_q a_s a_r | \Psi \rangle \\ &= \sum_{\mu,\nu} c^I_\mu c^{II}_\nu \langle D_\mu | a^\dagger_p a^\dagger_q a_s a_r | D_\nu \rangle, \end{aligned} \tag{6}$$

where p, q, r, and s are spin-orbital indices. Because the two simulations are uncorrelated, the two-body RDM in Eq. (6) becomes an unbiased one.

To calculate the spin-spin correlation, we need only the following 2-RDM elements:

$$\begin{aligned} \Gamma^{i\uparrow(\downarrow)j\uparrow(\downarrow)}_{i\uparrow(\downarrow)j\uparrow(\downarrow)} &= \langle \Psi | a^\dagger_{i,\uparrow(\downarrow)} a^\dagger_{j,\uparrow(\downarrow)} a_{j,\uparrow(\downarrow)} a_{i,\uparrow(\downarrow)} | \Psi \rangle \\ &= \langle \Psi | n_{i,\uparrow(\downarrow)} n_{j,\uparrow(\downarrow)} | \Psi \rangle, \\ \Gamma^{i\uparrow(\downarrow)j\downarrow(\uparrow)}_{i\uparrow(\downarrow)j\downarrow(\uparrow)} &= \langle \Psi | a^\dagger_{i,\uparrow(\downarrow)} a^\dagger_{j,\downarrow(\uparrow)} a_{j,\downarrow(\uparrow)} a_{i,\uparrow(\downarrow)} | \Psi \rangle \\ &= \langle \Psi | n_{i,\uparrow(\downarrow)} n_{j,\downarrow(\uparrow)} | \Psi \rangle, \\ \Gamma^{i\downarrow(\uparrow)j\uparrow(\downarrow)}_{i\uparrow(\downarrow)j\downarrow(\uparrow)} &= \langle \Psi | a^\dagger_{i,\uparrow(\downarrow)} a^\dagger_{j,\downarrow(\uparrow)} a_{j,\uparrow(\downarrow)} a_{i,\downarrow(\uparrow)} | \Psi \rangle. \end{aligned} \tag{7}$$

By using the following expressions of the local spin operators,

$$\begin{aligned} S^x_i &= \frac{1}{2}(a^\dagger_{i\uparrow} a_{i\downarrow} + a^\dagger_{i\downarrow} a_{i\uparrow}), \\ S^y_i &= \frac{i}{2}(a^\dagger_{i\downarrow} a_{i\uparrow} - a^\dagger_{i\uparrow} a_{i\downarrow}), \\ S^z_i &= \frac{1}{2}(n_{i\uparrow} - n_{i\downarrow}), \end{aligned} \tag{8}$$

the $\hat{S}^z$-spin correlation $\langle \hat{S}^z_i \cdot \hat{S}^z_j \rangle$ can be evaluated as

$$\begin{aligned} \langle \hat{S}^z_i \cdot \hat{S}^z_j \rangle &= \frac{1}{4}(\langle \Psi | n_{i,\uparrow} n_{j,\uparrow} | \Psi \rangle - \langle \Psi | n_{i,\uparrow} n_{j,\downarrow} | \Psi \rangle \\ &\quad - \langle \Psi | n_{i,\downarrow} n_{j,\uparrow} | \Psi \rangle + \langle \Psi | n_{i,\downarrow} n_{j,\downarrow} | \Psi \rangle) \\ &= \frac{1}{4}\left(\Gamma^{i\uparrow j\uparrow}_{i\uparrow j\uparrow} + \Gamma^{i\downarrow j\downarrow}_{i\downarrow j\downarrow} - \Gamma^{i\uparrow j\downarrow}_{i\uparrow j\downarrow} - \Gamma^{i\downarrow j\uparrow}_{i\downarrow j\uparrow}\right), \end{aligned} \tag{9}$$

and the total spin correlation function as

$$\begin{aligned} \langle \hat{\mathbf{S}}_i \cdot \hat{\mathbf{S}}_j \rangle &= \frac{1}{2}\left(\Gamma^{i\downarrow j\uparrow}_{i\uparrow j\downarrow} + \Gamma^{i\uparrow j\downarrow}_{i\downarrow j\uparrow}\right) \\ &\quad + \frac{1}{4}\left(\Gamma^{i\uparrow j\uparrow}_{i\uparrow j\uparrow} + \Gamma^{i\downarrow j\downarrow}_{i\downarrow j\downarrow} - \Gamma^{i\uparrow j\downarrow}_{i\uparrow j\downarrow} - \Gamma^{i\downarrow j\uparrow}_{i\downarrow j\uparrow}\right). \end{aligned} \tag{10}$$

For the special case when $\langle \hat{S}_z \rangle = 0$, the above expressions can be simplified to [40]

$$\langle \hat{S}^z_i \cdot \hat{S}^z_j \rangle = \frac{1}{2}\left(\Gamma^{i\uparrow j\uparrow}_{i\uparrow j\uparrow} - \Gamma^{i\uparrow j\downarrow}_{i\uparrow j\downarrow}\right) \tag{11}$$

and

$$\langle \hat{\mathbf{S}}_i \cdot \hat{\mathbf{S}}_j \rangle = \Gamma^{i\downarrow j\uparrow}_{i\uparrow j\downarrow} + \frac{1}{2}\left(\Gamma^{i\uparrow j\uparrow}_{i\uparrow j\uparrow} - \Gamma^{i\uparrow j\downarrow}_{i\uparrow j\downarrow}\right) \tag{12}$$

by using the relations $\Gamma^{i\uparrow j\uparrow}_{i\uparrow j\uparrow} = \Gamma^{i\downarrow j\downarrow}_{i\downarrow j\downarrow}$ and $\Gamma^{i\uparrow j\downarrow}_{i\uparrow j\downarrow} = \Gamma^{i\downarrow j\uparrow}_{i\downarrow j\uparrow}$. More details are presented in the Supplemental Material [44] (see, also, Refs. [1–3] therein).

III. RESULTS

Calculations are performed on three square lattices with tilted periodic boundary conditions, namely the 18-site lattice with lattice vectors $(3, 3), (3, -3)$, the 20-site lattice with lattice vectors $(4, -2), (-2, -4)$, and the 24-site lattice with lattice vectors $(5, 1), (-1, -5)$. The supercell of the 24-site lattice is not square, but the underlying lattice still is. This 24-site lattice has been discussed comprehensively by Betts [41] with regard to its finite-size properties, which are indeed favorable, having a low topological imperfection as defined by Betts. The above three tilted lattices are presented in [21] (see Fig. 1 therein).

A. The two-hole system

The two-hole system has been investigated in our previous work [21], where we find the total spin of the ground state is always zero for all the different lattices. This supports the early conclusions based on exact diagonalization [22] and analytical studies of arbitrarily large systems [19].

To check the performance of our algorithm, we first perform calculations on the 18-site lattice, where Lanczos-based ED results are available [42]. In Table I, the results of the spin-spin correlation, $\langle \hat{\mathbf{S}}(i) \cdot \hat{\mathbf{S}}(j) \rangle$, on the 18-site lattice for $U = 20$ and 40 are presented in comparison with the ED results. In our simulation we use a time step of $\tau = 0.001$, $N_w = 5 \times 10^7$ number of walkers and treat the 5×10^4 most populated states deterministically. As shown in Table I, the two results agree very well for different R (the distance between two different sites i and j).

In order to get a visual impression of the spatial spin distribution, we plot the pair correlation function $\langle \hat{S}_z(i)\hat{S}_z(j) \rangle$ for different interaction strengths and number of holes in a lattice cutout composed of four supercells, as presented in Figs. 1–3, respectively, for the 18-, 20-, and 24-site lattices. The lattice site i is set in the center of the cutout.

On the 18-site lattice, the spatial spin distribution in the half-filling case shows a clear antiferromagnetic pattern as shown in Fig. 1(d). For two-hole systems, we still find some antiferromagnetic features when U is not too large, as the cases shown in Figs. 1(a) and 1(b), where spins on neighboring sites are still antiparallel. However, when U is larger than a certain critical value (U_c), as presented in Fig. 1(c), the neighboring spins become parallel, and we find some kind of ferromagnetic domain structure. It is interesting to find that the critical U_c is very close to that of Nagaoka ferromagnetism in one-hole systems. We therefore do not try to determine these critical U_c values, but rather use those U_c's determined for the Nagaoka ferromagnetization as references. Such transitions of the spatial spin distribution patterns are also found on the 20- and 24-site lattices, see Fig. 2 and Fig. 3, where we also find ferromagnetic domains when U is large enough. When the lattice size increases, the size of the ferromagnetic domains becomes larger, and their shape changes.

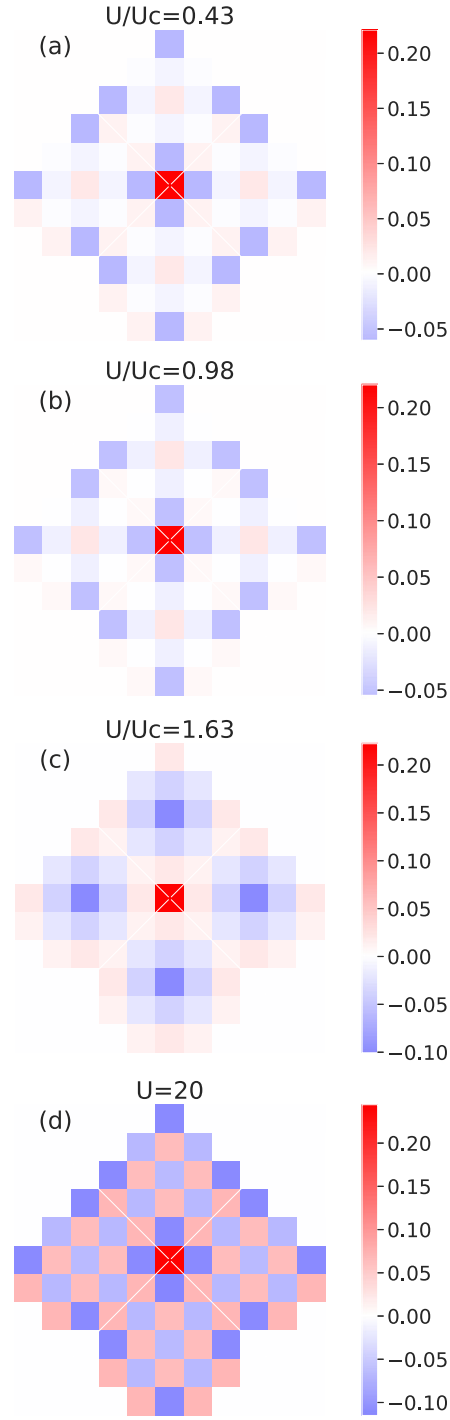

FIG. 1. Spatial spin distributions given by $\langle \hat{S}_z(i)\hat{S}_z(j) \rangle$ on the 18-site lattice for two-hole [(a)–(c)] and half-filled (d) systems. The critical interaction strength is $U_c = 92$ and the site i is set in the center.

The fact that critical U_c's are close to those of Nagaoka ferromagnetism in one-hole systems provides a physical picture that holes tend to separate from each other. This picture, originally suggested by Tian [43], is now tested and verified based on the analysis of SDs of the ground state. For the two-hole systems, we have also found that for large U's the binding energies are positive as shown in Fig. 4. The binding

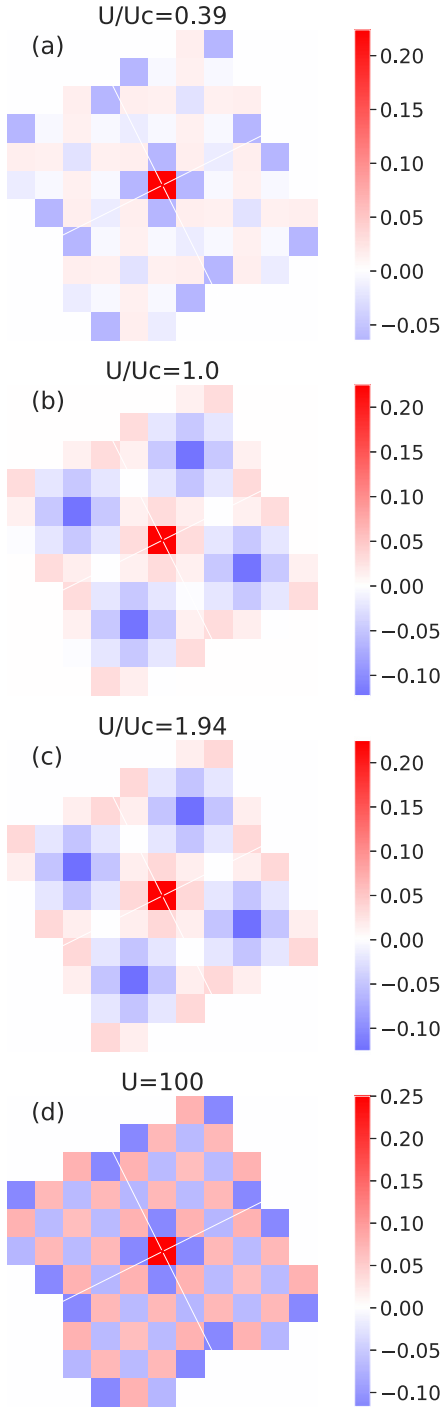

FIG. 2. Spatial spin distributions given by $\langle \hat{S}_z(i)\hat{S}_z(j)\rangle$ on the 20-site lattice for two-hole [(a)–(c)] and half-filled (d) systems. The critical interaction strength is $U_c = 103$.

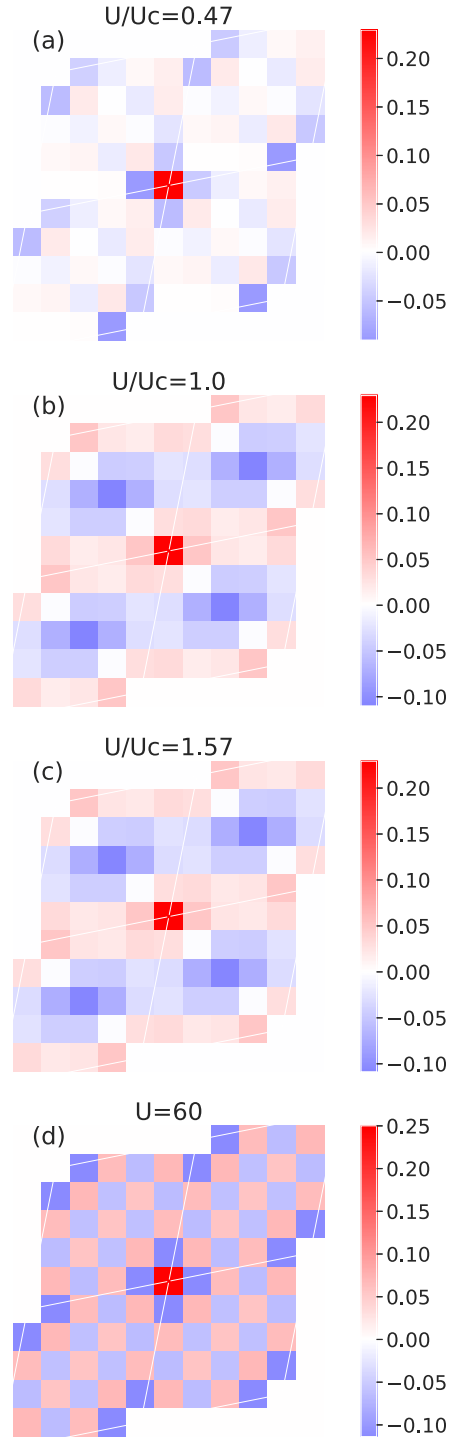

FIG. 3. Spatial spin distributions given by $\langle \hat{S}_z(i)\hat{S}_z(j)\rangle$ on the 24-site lattice for two-hole [(a)–(c)] and half-filled (d) systems. The critical interaction strength is $U_c = 127$.

energy of two holes is defined as $\delta = (E_2 - E_0) - 2(E_1 - E_0) = E_2 - 2E_1 + E_0$, where E_n is the ground-state energy of the n-hole system. The positive binding energy implies that two holes tend to separate, rather than to bind for large U's. In this case, it is reasonable to assume that each hole carries a halo of ferromagnetic texture.

To further confirm the picture of the hole separations we have looked at the spin distribution of the most populated SD in the ground state of the 20-site lattice. For $U = 200$, the spin distribution of the SD with highest weight is plotted in Fig. 5, where we find that the distance between two holes is the farthest, $\sqrt{10}$, and spins around each hole are the same. The analysis of the 8×10^5 most populated SDs shows that the most common hole distance is not $\sqrt{10}$, but $\sqrt{5}$ instead [as shown in Fig. 6(b)]. Similarly on the 24-site lattice, $\sqrt{5}$

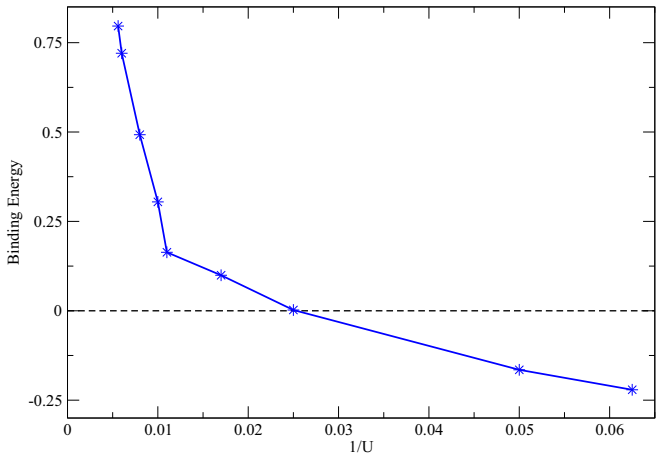

FIG. 4. Binding energy of two holes vs $1/U$ on 18 sites.

is the most common hole distance [Fig. 6(c)], and on the 18-site lattice, the distance 2 is slightly more common than $\sqrt{5}$ [Fig. 6(a)]. Ferromagnetic domains appear on finite lattices when holes are far away from each other. For systems with a fixed number of holes, the possibility of the formation of ferromagnetic domains increases with the system size, which means that the ferromagnetic domain structure favors a low hole density.

B. The three-hole system

For three-hole systems, we first study the possibility of partial spin polarization on lattices larger than 16 sites. As mentioned in the introduction, results of exact diagonalization (ED) based on an effective Hamiltonian [22] show that the total spin of the ground state on 8- and 16-site lattices is $\frac{3}{2}$ and $\frac{7}{2}$, respectively. If this partial spin polarization also exists for larger lattices, then for large enough U there would be a phase of ferrimagnetism (a mixed type of antiferromagnetism and ferromagnetism). To investigate this problem, we have mainly calculated ground-state energy as a function of total spin, $E(S)$, on 16- and 18-site lattices.

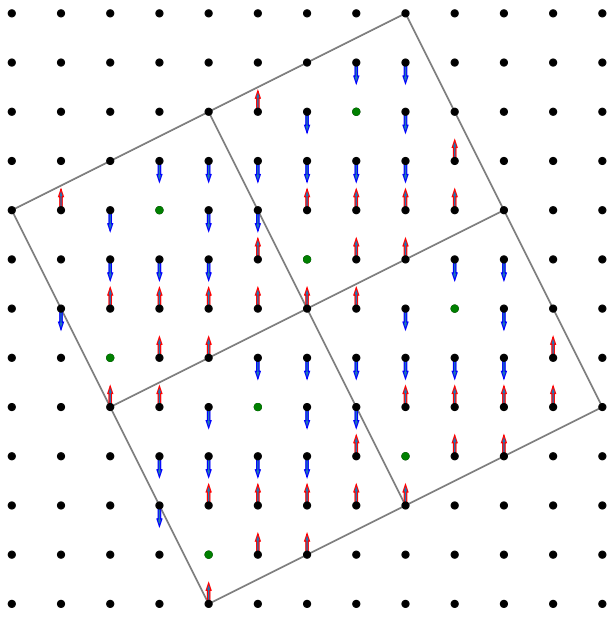

FIG. 5. Spin distributions of the Slater determinant with the most weight in the ground state of the 20-site lattice with two holes. The red (blue) arrows represent spin up (down), and the green dots represent a hole. The lattice cutout is composed of four supercells.

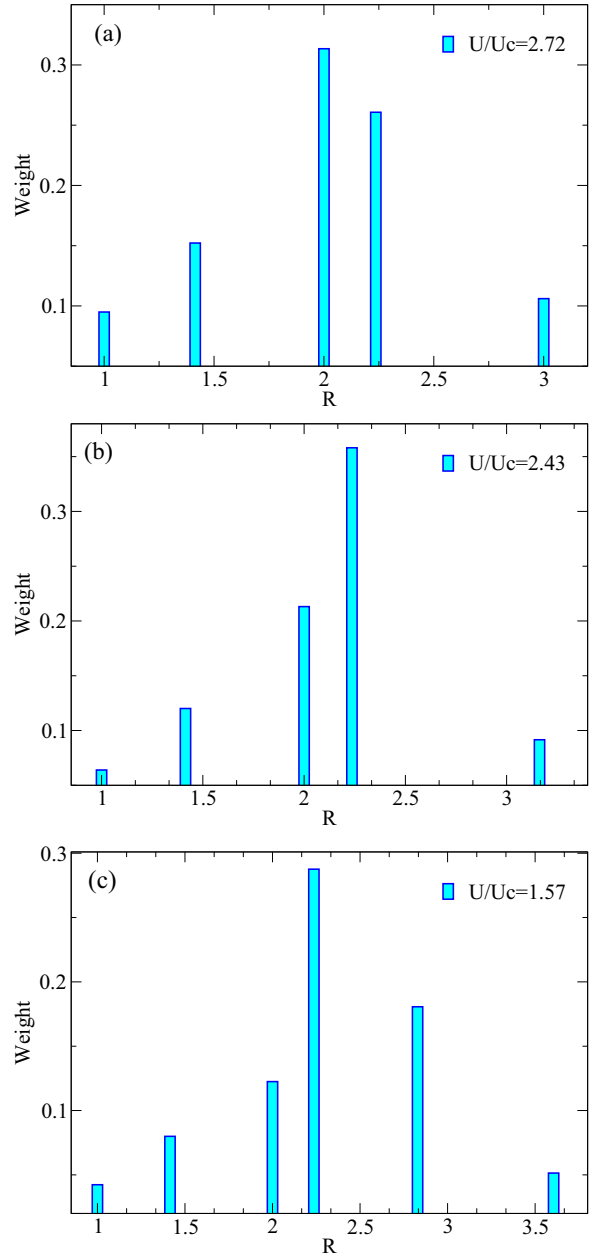

FIG. 6. Statistical distribution of the distance between two holes on 18-site (a), 20-site (b), and 24-site (c) lattices. The numbers of considered SDs in the ground-state wave function considered for the analysis are 5×10^5 (0.93% of total occupied SDs in the FCIQMC ground-state estimate), 8×10^5 (0.85% of occupied SDs), and 10^7 (0.76% of occupied SDs), respectively. Please note that the ground-state wave function is not normalized and the weight shown in the figure is a relative value.

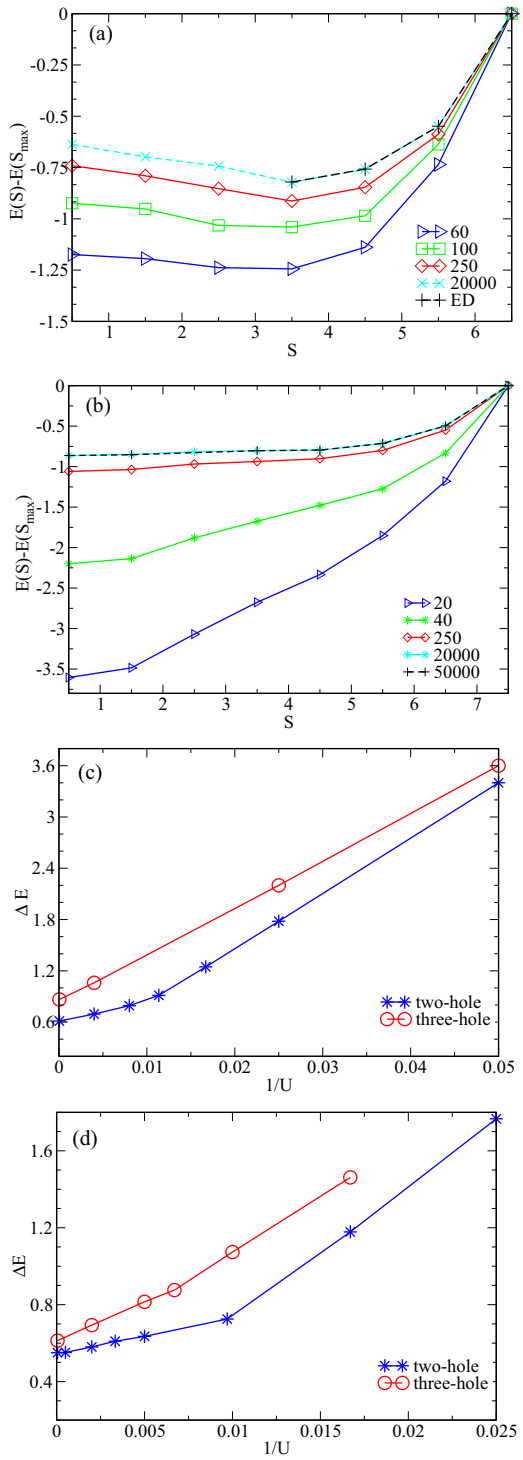

FIG. 7. $E(S) - E(S_{\max})$ versus S on 16-site (a) and 18-site (b) lattices with three holes, and the width of spin spectrum ΔE as the function of $1/U$ on 18-site (c) and 20-site (d) lattices, respectively.

In Fig. 7(a), the ground-state energy as a function of the total spin for the 16-site lattice is shown. The results are presented for different U's in comparison with the ED result for $U = \infty$ [22], according to Eq. (3). With increasing U, the $E(S)$ curves clearly converge to the ED result, and in fact the result at $U = 20\,000$ already coincides with the ED result. These results show a partial spin polarization at $S = \frac{7}{2}$ in the large-U regime. However, on the 18-site lattice, such a partial spin polarization does not exist for any U. In Fig. 7(b), the results of $E(S)$ are plotted for different U's for the 18-site lattice. The coincidence of the two curves at $U = 20\,000$ and $U = 50\,000$ indicates the convergence in the large-U limit. For any U the total spin of the ground state always takes the smallest value $S = 0.5$ and thus there is no partial spin polarization. Similar results are also obtained on the 20-site lattice, where we have only performed calculations for $U = 20\,000$. We therefore believe that the partial spin polarization result obtained in Ref. [22] is only a finite-size effect.

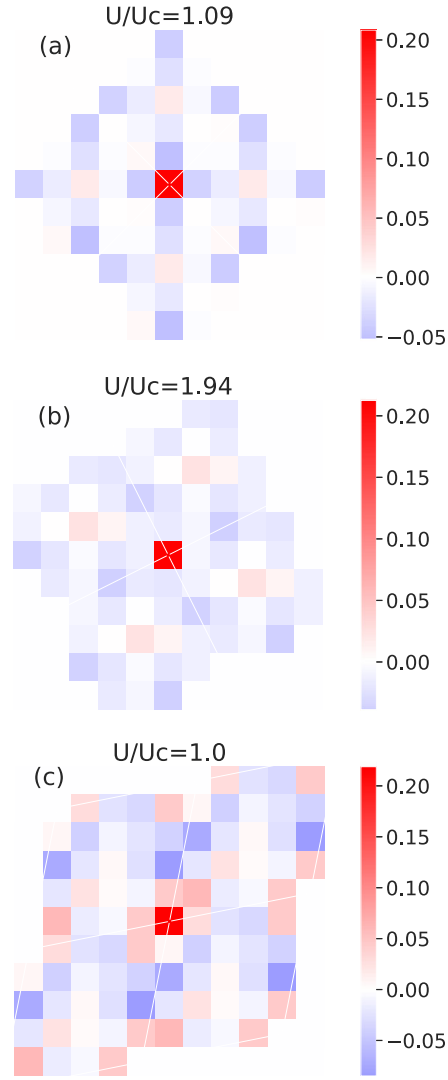

FIG. 8. The spatial spin distributions of the 18-, 20-, and 24-site lattices with three holes are provided in (a)–(c); U_c are the same as those in two-hole system.

To investigate the possibility of ferromagnetic domains in three-hole systems we have calculated the width of the spin spectrum $\Delta E = E_{\max} - E_{\min}$, where $E_{\max} = \max[E(S)]$, $E_{\min} = \min[E(S)]$ are the maximal and minimal values of the energy over all spin states for a given U. In our previous work [21], we find that for two-hole systems a clear change in the slope of $\Delta E(1/U)$ usually implies the formation of ferromagnetic domains. The widths of the spin

spectrum ΔE for three-hole systems on the 18- and 20-site lattices are plotted in Figs. 7(c) and 7(d), respectively, as functions of $1/U$, in comparison with those for two-hole systems. For three-hole systems, the curve of $\Delta E(1/U)$ for the 18-site lattice is simply a straight line, while for the 20-site lattice we see a small but clear change of slope. This indicates that on large enough lattices the three-hole systems can also have ferromagnetic domains in the large-U regime. To support this, we have also investigated spatial spin distributions of three-hole systems by calculating the spin-spin correlation functions. The spatial spin distributions are presented in Fig. 8, where ferromagnetic domains are found on 20- and 24-site lattices. Comparing with the ferromagnetic domains in two-hole systems, the extent of ferromagnetic domains is smaller in this case.

IV. CONCLUSION

The instability of Nagaoka ferromagnetism in the Hubbard model is studied for two- and three-hole systems on finite lattices. It is shown that the total spin of the ground state takes the minimal value $S = S_{\min}$, and there exists no partial spin polarization on lattices larger than 16 sites both on two- and three-hole systems. In the large-U regime ($U \geqslant U_c$, where U_c is the critical U of Nagaoka ferromagnetism in the one-hole system), we find the formation of ferromagnetic domains. Based on the analysis of binding energy and the statistical distance between two holes, we find a general feature of the ferromagnetic domain structure, with the holes tending to be far away from each other.

ACKNOWLEDGMENTS

S.Y. would like to extend her sincere gratitude to Nikolay Bogdanov and Giovanni Li Manni of the Max Planck Institute for Solid State Research, Youjin Deng of the University of Science and Technology of China, and Qianghua Wang of Nanjing University for participating in discussions and providing support. The authors gratefully acknowledge funding from the Max Planck Society. S.Y. is supported by the National Natural Science Foundation of China (Grants No. 11805103 and No. 11447204) and the Jiangsu Natural Science Foundation (Grant No. BK20190137).

[1] M. Qin, T. Schäfer, S. Andergassen, P. Corboz, and E. Gull, The Hubbard model: A computational perspective, Annu. Rev. Condens. Matter Phys. **13**, 275 (2022).

[2] D. J. Scalapino, A common thread: The pairing interaction for unconventional superconductors, Rev. Mod. Phys. **84**, 1383 (2012).

[3] M. Imada, A. Fujimori, and Y. Tokura, Metal-insulator transitions, Rev. Mod. Phys. **70**, 1039 (1998).

[4] T. Tohyama, Y. Inoue, K. Tsutsui, and S. Maekawa, Exact diagonalization study of optical conductivity in the two-dimensional Hubbard model, Phys. Rev. B **72**, 045113 (2005).

[5] D. Ohki, G. Matsuno, Y. Omori, and A. Kobayashi, Optical conductivity in a two-dimensional extended Hubbard model for an organic Dirac electron system α-(BEDT-TTF)$_2$I$_3$, Crystals **8**, 137 (2018).

[6] H. Dai, M. Cai, Q. Hao, Q. Liu, Y. Xing, H. Chen, X. Chen, X. Wang, H.-H. Fu, and J. Han, Nonlocal manipulation of magnetism in an itinerant two-dimensional ferromagnet, ACS Nano **16**, 12437 (2022).

[7] M. Holzmann and S. Moroni, Itinerant-Electron Magnetism: The Importance of Many-Body Correlations, Phys. Rev. Lett. **124**, 206404 (2020).

[8] Y. Nagaoka, Ferromagnetism in a narrow, almost half-filled *s* band, Phys. Rev. **147**, 392 (1966).

[9] D. J. Thouless, Exchange in solid ^{3}He and the Heisenberg Hamiltonian, Proc. Phys. Soc. **86**, 893 (1965).

[10] E. H. Lieb, Two Theorems on the Hubbard Model, Phys. Rev. Lett. **62**, 1201 (1989).

[11] H. Tasaki, Extension of Nagaoka's theorem on the large-U Hubbard model, Phys. Rev. B **40**, 9192 (1989).

[12] H. Tasaki, The Hubbard model: An introduction and selected rigorous results, J. Phys.: Condens. Matter **10**, 4353 (1998).

[13] I. Ivantsov, A. Ferraz, and E. Kochetov, Breakdown of the Nagaoka phase at finite doping, Phys. Rev. B **95**, 155115 (2017).

[14] A. Barbieri, J. A. Riera, and A. P. Young, Stability of the saturated ferromagnetic state in the one-band Hubbard model, Phys. Rev. B **41**, 11697 (1990).

[15] F. Becca and S. Sorella, Nagaoka Ferromagnetism in the Two-Dimensional Infinite-U Hubbard Model, Phys. Rev. Lett. **86**, 3396 (2001).

[16] L. Liu, H. Yao, E. Berg, S. R. White, and S. A. Kivelson, Phases of the Infinite-U Hubbard Model on Square Lattices, Phys. Rev. Lett. **108**, 126406 (2012).

[17] E. Müller-Hartmann, T. Hanisch, and R. Hirsch, Ferromagnetism of Hubbard models, Phys. B: Condens. Matter **186-188**, 834 (1993).

[18] P. Wurth, G. Uhrig, and E. Müller-Hartmann, Ferromagnetism of Hubbard models, Ann. Phys. **508**, 148 (1996).

[19] B. Doucot and X. G. Wen, Instability of the Nagaoka state with more than one hole, Phys. Rev. B **40**, 2719(R) (1989).

[20] Y. Fang, A. E. Ruckenstein, E. Dagotto, and S. Schmitt-Rink, Holes in the infinite-U Hubbard model: Instability of the Nagaoka state, Phys. Rev. B **40**, 7406(R) (1989).

[21] S. Yun, W. Dobrautz, H. Luo, and A. Alavi, Benchmark study of Nagaoka ferromagnetism by spin-adapted full configuration interaction quantum Monte Carlo, Phys. Rev. B **104**, 235102 (2021).

[22] J. A. Riera and A. P. Young, Ferromagnetism in the one-band Hubbard model, Phys. Rev. B **40**, 5285(R) (1989).

[23] W. Foulkes, L. Mitas, R. Needs, and G. Rajagopal, Quantum Monte Carlo simulations of solids, Rev. Mod. Phys. **73**, 33 (2001).

[24] H. Shi and S. Zhang, Some recent developments in auxiliary-field quantum Monte Carlo for real materials, J. Chem. Phys. **154**, 024107 (2021).

[25] G. H. Booth, A. J. W. Thom, and A. Alavi, Fermion Monte Carlo without fixed nodes: A game of life, death, and

annihilation in Slater determinant space, J. Chem. Phys. **131**, 054106 (2009).

[26] D. Cleland, G. H. Booth, and A. Alavi, Communications: Survival of the fittest: Accelerating convergence in full configuration-interaction quantum Monte Carlo, J. Chem. Phys. **132**, 041103 (2010).

[27] K. Guther, R. J. Anderson, N. S. Blunt, N. A. Bogdanov, D. Cleland, N. Dattani, W. Dobrautz, K. Ghanem, P. Jeszenszki, N. Liebermann, G. L. Manni, A. Y. Lozovoi, H. Luo, D. Ma, F. Merz, C. Overy, M. Rampp, P. K. Samanta, L. R. Schwarz, J. J. Shepherd, S. D. Smart, E. Vitale, O. Weser, G. H. Booth, and A. Alavi, NECI: *N*-electron configuration interaction with an emphasis on state-of-the-art stochastic methods, J. Chem. Phys. **153**, 034107 (2020).

[28] C. Overy, G. H. Booth, N. S. Blunt, J. S. Spencer, D. Cleland, and A. Alavi, Unbiased reduced density matrices and electronic properties from full configuration interaction quantum Monte Carlo, J. Chem. Phys. **141**, 244117 (2014).

[29] R. E. Thomas, G. H. Booth, and A. Alavi, Accurate *Ab Initio* Calculation of Ionization Potentials of the First-Row Transition Metals with the Configuration-Interaction Quantum Monte Carlo Technique, Phys. Rev. Lett. **114**, 033001 (2015).

[30] N. S. Blunt, G. H. Booth, and A. Alavi, Density matrices in full configuration interaction quantum Monte Carlo: Excited states, transition dipole moments, and parallel distribution, J. Chem. Phys. **146**, 244105 (2017).

[31] J. Paldus, Unitary-group approach to the many-electron correlation problem: Relation of Gelfand and Weyl tableau formulations, Phys. Rev. A **14**, 1620 (1976).

[32] I. Shavitt, Graph theoretical concepts for the unitary group approach to the many-electron correlation problem, Int. J. Quantum Chem. **12**, 131 (1977).

[33] I. Shavitt, Matrix element evaluation in the unitary group approach to the electron correlation problem, Int. J. Quantum Chem. **14**, 5 (1978).

[34] W. Dobrautz, S. D. Smart, and A. Alavi, Efficient formulation of full configuration interaction quantum Monte Carlo in a spin eigenbasis via the graphical unitary group approach, J. Chem. Phys. **151**, 094104 (2019).

[35] W. Dobrautz, O. Weser, N. A. Bogdanov, A. Alavi, and G. Li Manni, Spin-pure stochastic-CASSCF via GUGA-FCIQMC applied to iron-sulfur clusters, J. Chem. Theory Comput. **17**, 5684 (2021).

[36] G. L. Manni, W. Dobrautz, and A. Alavi, Compression of spin-adapted multiconfigurational wave functions in exchange-coupled polynuclear spin systems, J. Chem. Theory Comput. **16**, 2202 (2020).

[37] G. Li Manni, W. Dobrautz, N. A. Bogdanov, K. Guther, and A. Alavi, Resolution of low-energy states in spin-exchange transition-metal clusters: Case study of singlet states in $[Fe(III)_4S_4]$ cubanes, J. Phys. Chem. A **125**, 4727 (2021).

[38] K. A. Chao, J. Spałek, and A. M. Oleś, Canonical perturbation expansion of the Hubbard model, Phys. Rev. B **18**, 3453 (1978).

[39] A. B. Harris and R. V. Lange, Single-particle excitations in narrow energy bands, Phys. Rev. **157**, 295 (1967).

[40] W. Kutzelnigg, K. Shamasundar, and D. Mukherjee, Spin-free formulation of reduced density matrices, density cumulants and generalised normal ordering, Mol. Phys. **108**, 433 (2010).

[41] D. D. Betts, H. Q. Lin, and J. S. Flynn, Improved finite-lattice estimates of the properties of two quantum spin models on the infinite square lattice, Can. J. Phys. **77**, 353 (1999).

[42] F. Becca, A. Parola, and S. Sorella, Ground-state properties of the Hubbard model by Lanczos diagonalizations, Phys. Rev. B **61**, R16287 (2000).

[43] G. Tian, Stability of the Nagaoka state in the one-band Hubbard model, Phys. Rev. B **44**, 4444 (1991).

[44] See Supplemental Material at http://link.aps.org/supplemental/10.1103/PhysRevB.107.064405 for details of spin correlations functions. We also present there some results of ground state energies for the two-hole and three-hole sectors on the 20-site lattice.